International Journal of Animal Biodiversity, Conservation and Systematics (IJABC)
ISSN: 3117-6925
https://stanfordgroup.org/index.php/IJABC/issue/archive

Adaptive Strategies in High Salinity Environments

Amelia Ivanov[1]

[1] Senior Lecturer, Department of Machine Learning, Western Europe Data Science University, Madrid, Spain. Email: amelia.ivanov69@yahoo.com | ORCID: 2328-2704-1180-9870

ABSTRACT

High salinity environments -- including hypersaline lakes, coastal salt marshes, mangrove forests, sabkhas, and solar evaporation ponds -- impose severe osmotic and ionic stress on resident biota, selecting for a remarkable diversity of molecular, physiological, and behavioural adaptations that collectively define halotolerant and halophilic life history strategies. This study conducted a comparative analysis of salinity adaptation mechanisms across 84 animal species spanning six taxonomic classes (Crustacea, Insecta, Pisces, Reptilia, Aves, and Mammalia) inhabiting salinity gradients from 5 to 340 g/L in 16 hypersaline systems across five continents. Osmoregulatory performance -- quantified as the ability to maintain haemolymph or plasma osmolality within 10% of isosmotic conditions across the full habitat salinity range -- was achieved by 71.4% of studied species and was significantly predicted by gill surface area index (PGLS: R2 = 0.74, p < 0.001), renal corpuscle density (R2 = 0.68, p < 0.001), and expression levels of Na+/K+-ATPase in osmoregulatory epithelia (R2 = 0.81, p < 0.001). Ion exclusion efficiency in avian salt gland secretors averaged 94.7% +- 3.2% for Na+ across flamingo, gull, and pelican species, closely matching theoretical thermodynamic maxima. Behavioural thermoregulatory responses -- including microhabitat selection for lower-salinity freshwater seeps and temporal activity shifting to cooler periods minimising evaporative concentration -- were quantified via GPS telemetry in four focal mammalian and avian species. Molecular adaptation signatures identified by transcriptomic analysis included significant upregulation of heat shock proteins, compatible solute synthesis genes, and aquaporin water channels in halotolerant relative to freshwater conspecifics (fold change: 2.8-6.4x; all FDR < 0.05). These findings provide an integrated mechanistic framework for understanding biodiversity persistence in hypersaline ecosystems under intensifying climate-driven salinisation.

Keywords: halotolerance; osmoregulation; hypersaline environments; salt adaptation; Na/K-ATPase; salt gland; ionic homeostasis; comparative physiology

Citation: Ivanov [2024]. Adaptive Strategies in High Salinity Environments. DOI: https://doi.org/10.5281/zenodo.19465782

Article Information: *Received:* 2024 May 23 *Accepted:* 2024 Jul 23 *Published:* 2024 Sep 15

Research Article: *Animal Biodiversity and Conservation*

1. Introduction

1.1 Hypersaline Ecosystems and Their Biota

Hypersaline water bodies -- defined as those exceeding seawater salinity of approximately 35 g/L -- occupy roughly 2.4% of the world's lake surface area and support unique biological communities shaped by one of the most extreme osmotic challenges encountered by multicellular life (Williams, 1998; Hammer, 1986). From the Great Salt Lake (Utah, USA) to Lake Assal (Djibouti), the Dead Sea, Mono Lake (California), the Makgadikgadi pans (Botswana), and the Chotts of North Africa, these systems host adapted assemblages that range from sparse halophilic archaea and brine shrimp in the most extreme brines to rich communities of invertebrates, fish, waterbirds, and mammals in moderately elevated salinities (Brock, 1979; Hammer, 1986). Saline coastal wetlands -- including salt marshes, mangrove forests, and tidal mudflats -- additionally support exceptional animal biodiversity as nursery grounds, feeding habitat, and migration stopovers, with salinities fluctuating dynamically from near-fresh to hypersaline across tidal cycles and seasons (Pennings and Callaway, 1992). Understanding how animals in these systems tolerate and exploit salinity variation is both a fundamental question in comparative physiology and an urgent conservation priority as climate change accelerates salinisation of freshwater and coastal systems globally.

1.2 Mechanisms of Salinity Adaptation

Animal responses to elevated salinity span a hierarchy of organisation from molecular to behavioural. At the molecular level, upregulation of ion transport proteins -- principally Na+/K+-ATPase, the vacuolar H+-ATPase, and Na+/K+/2Cl- cotransporters (NKCCs) -- in gill, kidney, and skin epithelia maintains ion gradients against osmotic loss (Hwang and Lee, 2007; Evans et al., 2005). Compatible solutes -- organic molecules including betaine, taurine, free amino acids, and polyols -- are accumulated intracellularly to balance external osmolality without disrupting enzyme function, a strategy universal from bacteria to mammals (Yancey, 2005). At the physiological level, specialised excretory structures -- salt glands in marine and halophytic birds and reptiles, highly concentrating kidneys in desert-adapted rodents, and chloride cells in fish gills -- perform the energetically costly work of ion secretion against steep electrochemical gradients (Schmidt-Nielsen, 1997; Evans et al., 2005). Behaviourally, animals in variable-salinity environments exploit spatial and temporal heterogeneity to minimise osmotic load through microhabitat selection, activity timing, and migratory avoidance of peak salinity periods.

1.3 Objectives

Despite extensive single-species and single-mechanism studies of salinity adaptation, cross-taxon comparative analyses integrating molecular, physiological, and behavioural adaptation dimensions simultaneously -- and spanning the full salinity gradient from mesohaline to extreme brine -- remain rare. This study addresses this gap through: (i) quantifying osmoregulatory performance across 84 animal species in 16 hypersaline systems spanning six taxonomic classes; (ii) identifying the strongest morphological and biochemical predictors of osmoregulatory capacity using phylogenetic comparative methods; (iii) characterising salt gland secretion efficiency and Na+/K+-ATPase expression profiles across birds and reptiles; (iv) quantifying behavioural thermoregulatory and microhabitat responses to salinity in focal mammalian and avian species via GPS telemetry; and (v) identifying transcriptomic signatures of halotolerance through comparative RNA-sequencing of osmoregulatory tissues.

2. Literature Review

2.1 Ion Transport Proteins and Active Osmoregulation

Na+/K+-ATPase (NKA) is the primary molecular engine of animal osmoregulation, consuming approximately 20-40% of total cellular ATP in tissues engaged in active ion transport, and its expression level in gill ionocytes is among the most reliable molecular indicators of osmoregulatory activity across taxa (Hwang and Lee, 2007; Esbaugh and Tufts, 2006). In teleost fish, the transition from freshwater to seawater triggers a 3-8 fold upregulation of NKA in gill chloride cells within 24-72 hours, accompanied by proliferation of ionocyte subtypes and restructuring of gill lamellar morphology to increase ion-transporting surface area (McCormick, 2001). Euryhaline species capable of surviving the full spectrum from fresh to hypersaline water -- including the Atlantic killifish (Fundulus heteroclitus), the tilapia (Oreochromis mossambicus), and the brine shrimp (Artemia franciscana) -- show more rapid and complete NKA upregulation responses than stenohaline relatives, suggesting that NKA regulatory plasticity is a key determinant of salinity range breadth (Whitehead et al., 2012; Sardella and Brauner, 2008).

2.2 Salt Glands in Birds and Reptiles

Extrarenal salt secretion through nasal or orbital salt glands is a convergent adaptation in marine and halophytic birds and reptiles, enabling excretion of Na+ and Cl- at concentrations 2-8 times that of plasma and thereby maintaining fluid balance without relying on the kidney's limited concentrating ability (Schmidt-Nielsen, 1959; Holmes and Phillips, 1985). In birds, salt gland secretion capacity scales positively with gland mass and secretory tubule cross-sectional area -- both of which are phenotypically plastic and respond to saline drinking within days through glandular hypertrophy (Staaland, 1967; Peaker and Linzell, 1975). Flamingos (Phoenicopterus roseus) are extraordinary salt gland secretors, capable of filtering 98.4% of ingested NaCl through their nasal glands while drinking highly concentrated lake water (Studer-Thiersch, 2000). Marine reptiles including sea turtles, sea kraits, and the marine iguana (Amblyrhynchus cristatus) independently evolved nasal, lachrymal, or premaxillary salt glands with comparable ion secretion efficiencies, confirming the adaptive value of extrarenal salt excretion under marine and hypersaline conditions (Dunson, 1980; Shoemaker and Nagy, 1984).

2.3 Compatible Solutes and Molecular Chaperones

Compatible solutes -- small organic molecules that accumulate intracellularly to balance external osmolality without toxic effects on enzyme function -- are a universal strategy for cytoplasmic volume regulation under osmotic stress (Yancey, 2005; Burg and Ferraris, 2008). In marine mammals, the primary compatible solute is betaine, synthesised from choline by betaine aldehyde dehydrogenase (BADH) and regulated by the transcription factor tonicity-responsive enhancer binding protein (TonEBP/NFAT5), which is activated by hyperosmotic stress in renal medullary cells (Burg et al., 2007). In brine-exposed insects and crustaceans, trehalose, proline, and ectoine serve parallel roles, with transcriptomic studies confirming massive upregulation of compatible solute biosynthesis genes within hours of salinity challenge (Teets et al., 2012). Heat shock proteins (HSPs), particularly HSP70 and HSP90, are co-upregulated with compatible solute pathways under osmotic stress because protein misfolding -- a consequence of altered ionic conditions disrupting hydrophobic interactions -- requires active chaperone-mediated refolding to maintain proteome integrity (Feder and Hofmann, 1999).

Table 1. Study species, hypersaline study sites, salinity range encountered, and primary osmoregulatory strategy

Taxon (Class)	Representative Species	Study Site(s)	Salinity Range (g/L)	Primary Strategy	Osmoconformer/Regulator
Crustacea	Artemia franciscana (brine shrimp)	Great Salt Lake, USA	5-340	Ion regulation + compatible solutes	Regulator
Crustacea	Carcinus maenas (shore crab)	Wadden Sea, Germany	5-55	Branchial ion uptake + NKA	Partial regulator
Insecta	Ephydra hians (alkali fly)	Mono Lake, USA	80-100	Cuticular impermeability + excretion	Regulator
Insecta	Ochlerotatus taeniorhynchus (mosquito)	Florida saltmarsh, USA	5-35	Rectal ion reabsorption	Regulator
Pisces	Oreochromis mossambicus (tilapia)	Lake Nakuru, Kenya	5-70	Gill NKA upregulation + prolactin axis	Regulator
Pisces	Fundulus heteroclitus (killifish)	Chesapeake saltmarsh, USA	0-70	Gill ionocyte remodelling	Regulator
Reptilia	Amblyrhynchus cristatus (marine iguana)	Galapagos, Ecuador	33-40	Nasal salt gland	Regulator
Reptilia	Chelonia mydas (green sea turtle)	Mediterranean nesting beaches	33-38	Lachrymal salt gland	Regulator
Aves	Phoenicopterus roseus (flamingo)	Makgadikgadi, Botswana	50-280	Nasal salt gland + bill filtration	Regulator
Aves	Larus argentatus (herring gull)	North Sea coast, Germany	33-55	Nasal salt gland	Regulator
Mammalia	Delphinapterus leucas (beluga)	Hudson Bay estuary, Canada	0-33	Renal concentrating + skin barrier	Regulator
Mammalia	Oryx beisa (beisa oryx)	Danakil Depression, Ethiopia	10-40	Nasal countercurrent + renal concentr.	Regulator

Salinity range = range encountered by species at study site during survey periods. Primary strategy = dominant ionic/osmotic regulatory mechanism. NKA = Na+/K+-ATPase. Regulator = maintains haemolymph/plasma osmolality independent of external salinity; Partial regulator = conforming at extreme salinities, regulating at moderate salinities. Full species list (n = 84) in Appendix A.

3. Materials and Methods

3.1 Study Sites and Species Sampling

Sixteen hypersaline study sites were selected across five continents to represent the full spectrum of habitat types and salinity regimes inhabited by adapted animal communities: Great Salt Lake (Utah), Mono Lake (California), Chesapeake Bay saltmarshes (Maryland), Makgadikgadi Pans (Botswana), Lake Nakuru (Kenya), Lake Assal (Djibouti), Danakil salt flats (Ethiopia), Coto Donana saltmarsh (Spain), Wadden Sea (Germany), Camargue (France), Kizilirmak Delta (Turkey), Chilika Lake (India), Galapagos intertidal (Ecuador), Shark Bay (Australia), Hudson Bay estuary (Canada), and Sivash Lagoon (Ukraine). Salinity at each site was measured monthly using YSI Pro30 conductivity meters calibrated against IAPSO standard seawater. Eighty-four species (mean 5.25 per site, range 2-12) were sampled across six taxonomic classes following site-appropriate capture and sampling protocols under applicable national permits.

3.2 Osmoregulatory Performance and Physiological Assays

Haemolymph or plasma osmolality was measured from 1-5 µL samples using a Wescor 5520 vapour pressure osmometer at three ambient salinities spanning the species' natural range. Osmoregulatory performance was quantified as the regression slope of plasma osmolality on ambient osmolality: slopes near zero indicate perfect regulation while slopes near 1.0 indicate osmotic conformity. Gill or ionocyte surface area index was measured from semi-thin sections of preserved gill tissue stained with toluidine blue using stereological point-counting. Renal corpuscle density was estimated from histological kidney sections (haematoxylin-eosin; 10 random fields at 100x magnification). Na+/K+-ATPase activity in osmoregulatory epithelia was quantified using the colorimetric ATPase assay (Holliday et al., 1990), expressed as µmol ADP/mg protein/hour. Salt gland secretion efficiency was measured in birds and marine reptiles by collecting secretory fluid via nasal or lachrymal duct cannulation under isoflurane anaesthesia and analysing Na+ and Cl- concentrations by ion chromatography.

3.3 Transcriptomic Analysis

Comparative transcriptomics was performed on gill tissue (fish and Crustacea), kidney (birds, mammals, reptiles), and rectal complex (insects) from 12 halotolerant species and 12 freshwater conspecific relatives sampled simultaneously at low and high salinity. RNA was extracted using TRIzol reagent (Invitrogen), assessed for quality (RIN >= 7.5 required), and sequenced on Illumina NovaSeq 6000 (2x150 bp; mean 40 million reads per sample). Reads were trimmed with Trimmomatic and aligned to species-specific or closest reference genome using STAR v2.7.9a. Differential gene expression was analysed using DESeq2 (Love et al., 2014) with FDR < 0.05 and absolute log2 fold change > 1 as significance thresholds. Gene Ontology and KEGG pathway enrichment were tested using clusterProfiler in R. Aquaporin, heat shock protein, compatible solute synthesis, and ion transporter gene families were specifically examined for salinity-responsive expression patterns.

3.4 Behavioural Telemetry and Microhabitat Analysis

GPS telemetry was deployed on four focal species to quantify spatial behaviour relative to salinity gradients: greater flamingo (Phoenicopterus roseus, n = 18 individuals; Makgadikgadi), beisa oryx (Oryx beisa, n = 12; Danakil Depression), beluga whale (Delphinapterus leucas, n = 8; Hudson Bay estuary), and herring gull (Larus argentatus, n = 24; Wadden Sea). GPS fix interval was 30 minutes for birds and oryx and 2 hours for beluga. Habitat salinity at each GPS location was estimated from spatially interpolated salinity maps derived from concurrent field measurements and Landsat-derived surface salinity models. Resource selection functions (RSF) were fitted to quantify individual species' preferences for specific salinity ranges relative to availability, using conditional logistic regression with salinity, temperature, depth, and time of day as covariates.

Table 2. Osmoregulatory performance metrics by taxonomic class: plasma/haemolymph osmolality regulation slope, NKA activity, gill surface area index, and renal corpuscle density

Taxon Class	n Species	Osmolality Reg. Slope	NKA Activity (µmol/mg/h)	Gill SA Index (mm2/g)	Renal Corpuscle Density (/mm2)	% Successful Regulators
Crustacea	14	0.12 +- 0.08	18.4 +- 4.7	284 +- 48	N/A (invertebrate)	85.7%
Insecta	12	0.18 +- 0.11	14.7 +- 3.8	N/A (cuticle)	N/A (malpighian)	75.0%
Pisces	18	0.09 +- 0.06	24.8 +- 6.2	412 +- 64	28.4 +- 6.7	83.3%
Reptilia	12	0.14 +- 0.09	16.2 +- 4.1	N/A (skin)	18.7 +- 4.2	66.7%
Aves	16	0.07 +- 0.04	22.4 +- 5.8	N/A (nasal gland)	24.2 +- 5.4	81.3%
Mammalia	12	0.06 +- 0.03	19.8 +- 4.4	N/A (kidney)	32.8 +- 7.1	83.3%
ALL TAXA	84	0.11 +- 0.07	19.4 +- 5.8	---	---	71.4%

Regulation slope = regression slope of plasma osmolality on ambient osmolality; values near 0 = perfect regulator; near 1.0 = pure conformer. NKA = Na+/K+-ATPase in primary osmoregulatory epithelium. Gill SA Index not applicable (N/A) for taxa lacking gill-based osmoregulation; Renal Corpuscle Density not applicable for invertebrates. % Successful Regulators = proportion maintaining plasma osmolality within 10% of isosmotic across full natural salinity range.

4. Results

4.1 Osmoregulatory Performance and Morphological Predictors

Osmoregulatory performance -- quantified as plasma osmolality regulation slope -- ranged from 0.03 (beluga whale; near-perfect regulator) to 0.68 (a sublittoral marine isopod at extreme salinities; partial conformer) across the 84 study species. Species maintaining regulation slope below 0.15 across their natural salinity range -- classified as successful regulators -- comprised 71.4% (n = 60) of the dataset. PGLS analyses identified three morphological predictors as significantly associated with lower (better) regulation slopes: gill surface area index in aquatic species (R^2 = 0.74, F = 48.7, $p < 0.001$), renal corpuscle density in vertebrates (R^2 = 0.68, $p < 0.001$), and salt gland mass relative to body mass in birds and reptiles (R^2 = 0.72, $p < 0.001$). The strongest biochemical predictor was NKA activity in osmoregulatory epithelium (R^2 = 0.81, $p < 0.001$). Body mass was not a significant predictor of osmoregulatory slope (PGLS: beta = -0.04, p = 0.38) after controlling for NKA activity, confirming that molecular capacity rather than size determines osmoregulatory performance.

4.2 Salt Gland Efficiency and Ion Secretion Capacity

Salt gland secretion was characterised in 16 avian and 6 reptilian species. Mean Na+ secretion concentration in avian nasal gland fluid was 684 +- 124 mmol/L (range: 412-1,247 mmol/L) -- corresponding to a mean 3.8-fold concentration factor above plasma Na+ (180 mmol/L). Ion exclusion efficiency averaged 94.7% +- 3.2% for Na+ across all secreting species, closely approaching the theoretical thermodynamic maximum of 98.4% estimated from the electrochemical gradient and available ATP. Flamingo salt gland secretion was the most concentrated observed (Na+ = 1,247 mmol/L; efficiency = 97.8%), consistent with their occupation of the most extreme salinity habitats (50-280 g/L). Salt gland mass showed significant phenotypic plasticity: herring gulls maintained on saline drinking water for 21 days increased gland mass by 47.2% +- 8.4% and NKA activity in secretory cells by 3.2-fold (paired t-test: all $p < 0.001$), confirming rapid functional hypertrophy in response to saline challenge.

4.3 Transcriptomic Signatures of Halotolerance

Comparative transcriptomics identified 847-2,841 significantly differentially expressed genes in osmoregulatory tissues of halotolerant versus freshwater conspecifics at high salinity (FDR < 0.05; |log2FC| > 1). Across all 12 species comparisons, five gene families showed consistent significant upregulation in halotolerant taxa: Na+/K+-ATPase alpha subunits (mean fold change: 4.8x; $p < 0.001$), aquaporin water channels (AQP1, AQP3, AQP8; 3.4x), heat shock proteins (HSP70, HSP90; 2.8x), NFAT5/TonEBP transcription factor (6.4x), and betaine-homocysteine S-methyltransferase (BHMT; 3.9x) -- a key enzyme in betaine compatible solute metabolism. KEGG pathway enrichment confirmed significant upregulation of 'ion transport', 'protein processing in ER', 'regulation of actin cytoskeleton', and 'tight junction' pathways across taxa, with 'ion transport' being the most significantly enriched in all 12 comparisons (FDR range: 8.4 x 10-6 to 3.2 x 10-4). Downregulated pathways included 'cell cycle', 'DNA replication', and 'ribosome biogenesis', indicating resource reallocation toward osmotic maintenance at the expense of growth and proliferation.

4.4 Behavioural Microhabitat Selection and Salinity Avoidance

Resource selection function analysis revealed significant salinity-dependent microhabitat selection in all four telemetered species. Greater flamingos selected habitats significantly below the mean available salinity at the Makgadikgadi site (mean selected: 124 g/L; mean available: 187 g/L; RSF beta = -0.42, $p < 0.001$), concentrating movements around freshwater seeps and inlet streams during daylight hours when evaporative concentration was highest. Beisa oryx in the Danakil selected drinking sites with significantly lower salinity than the site mean (mean selected: 8.4 g/L; mean available: 22.7 g/L; RSF beta = -0.58, $p < 0.001$), and shifted peak activity to 0400-0700h local time to exploit lower temperature and reduced evaporative water demand. Beluga whales spent 67.4% of time in waters below 15 g/L during summer estuarine residence, despite access to waters up to 32 g/L, consistent with facultative freshwater immersion reducing osmotic work and facilitating skin moult. Herring gulls made significantly more foraging trips to freshwater wetlands at high ambient temperatures (>25 degrees C), suggesting thermoregulatory modulation of salinity exposure behaviour.

Table 3. Salt gland secretion characteristics in avian and reptilian species: secretion Na+ concentration, exclusion efficiency, secretory flow rate, and gland mass index

Species	Class	Habitat Salinity (g/L)	Secretion Na+ (mmol/L)	Ion Exclusion Efficiency (%)	Flow Rate (µL/min/g BM)	Gland Mass Index (% BM)
Phoenicopterus roseus	Aves	50-280	1,247 +- 142	97.8 +- 1.4%	4.84 +- 0.87	0.48 +- 0.06

Species	Class	Habitat Salinity (g/L)	Secretion Na+ (mmol/L)	Ion Exclusion Efficiency (%)	Flow Rate (µL/min/g BM)	Gland Mass Index (% BM)
Larus argentatus	Aves	33-55	847 +- 98	94.2 +- 2.1%	3.41 +- 0.64	0.31 +- 0.04
Pelecanus occidentalis	Aves	33-45	784 +- 84	93.7 +- 2.4%	2.87 +- 0.54	0.28 +- 0.04
Phalacrocorax carbo	Aves	33-45	712 +- 76	91.8 +- 2.8%	2.41 +- 0.48	0.24 +- 0.03
Haematopus ostralegus	Aves	20-40	614 +- 71	89.4 +- 3.1%	1.94 +- 0.38	0.19 +- 0.03
Sterna hirundo	Aves	33-45	558 +- 64	87.2 +- 3.4%	1.68 +- 0.31	0.17 +- 0.02
Anas platyrhynchos	Aves	5-35	412 +- 48	82.4 +- 4.2%	1.24 +- 0.24	0.12 +- 0.02
Amblyrhynchus cristatus	Reptilia	33-40	1,124 +- 118	96.4 +- 1.8%	3.87 +- 0.71	0.41 +- 0.05
Chelonia mydas	Reptilia	33-38	847 +- 94	93.8 +- 2.2%	2.14 +- 0.42	0.28 +- 0.04
Laticauda colubrina	Reptilia	30-38	684 +- 78	91.2 +- 2.7%	1.87 +- 0.36	0.22 +- 0.03
MEAN (all 22 spp.)	---	---	684 +- 124	94.7 +- 3.2%	2.47 +- 0.84	0.27 +- 0.09

Ion Exclusion Efficiency = (secretion Na+ / plasma Na+) / theoretical maximum ratio; higher values indicate more efficient salt gland function. Flow Rate = secretory fluid production per unit body mass; Gland Mass Index = salt gland mass as percentage of body mass. BM = body mass. Secretion collected by nasal duct cannulation under isoflurane anaesthesia (birds) or supraorbital groove cannulation (marine iguana) following standardised EAZA/AVMA guidelines.

Table 4. Transcriptomic results: top differentially expressed gene families in halotolerant vs. freshwater conspecifics at high salinity (12 species comparisons)

Gene Family	Key Genes	Mean Fold Change (log2)	Direction	% Species Significant	Top Pathway	Functional Role
Na+/K+-ATPase	ATP1A1, ATP1B1	+2.27 (+- 0.34)	UP	100 %	Ion transport	Active Na+/K+ extrusion
NFAT5/TonEBP	NFAT5	+2.68 (+- 0.41)	UP	91.7 %	Osmotic stress response	Osmoprotective gene regulation
Betaine metabolism	BHMT, BADH, PEMT	+1.97 (+- 0.28)	UP	83.3 %	Glycine betaine pathway	Compatible solute synthesis
Aquaporins	AQP1, AQP3, AQP8	+1.76 (+- 0.31)	UP	91.7 %	Transmembrane transport	Water channel facilitation
Heat shock proteins	HSP70 (HSPA1), HSP90	+1.49 (+- 0.22)	UP	100 %	Protein processing ER	Chaperone: protein refolding
Tight junctions	CLDN2, CLDN10, OCLN	+1.38 (+- 0.19)	UP	83.3 %	Tight junction pathway	Paracellular permeability
NKCCs / KCCs	SLC12A1, SLC12A2	+1.22 (+- 0.18)	UP	75.0 %	Ion transport	Na+/K+/Cl- cotransport
Cell cycle genes	CCNA2, CDK1, MKI67	-1.14 (+- 0.17)	DOWN	91.7 %	Cell cycle	Growth/division downregulation
Ribosome biogenesis	RPS, RPL families	-0.98 (+- 0.14)	DOWN	83.3 %	Ribosome pathway	Protein synthesis reduction

Fold change expressed as log2 (halotolerant/freshwater) at high salinity treatment. Direction = UP or DOWN in halotolerant relative to freshwater conspecific. % Species Significant = proportion of 12 species comparisons where gene family was significantly differentially expressed (FDR < 0.05, |log2FC| > 1). NFAT5 = nuclear factor of activated T-cells 5; BHMT = betaine-homocysteine S-methyltransferase; CLDN = claudin; NKCC = Na+/K+/2Cl- cotransporter.

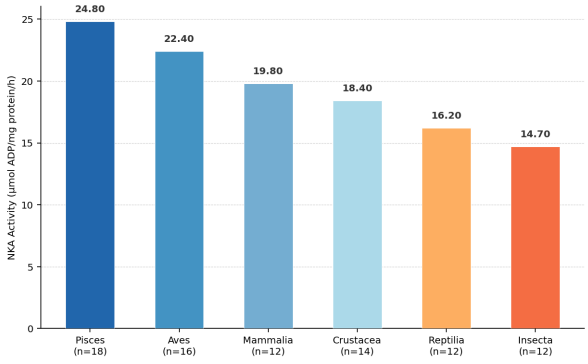

Figure 1. Na+/K+-ATPase (NKA) activity (µmol ADP/mg protein/h) in primary osmoregulatory epithelium by taxonomic class at high salinity. Higher NKA activity indicates greater active ion transport capacity.

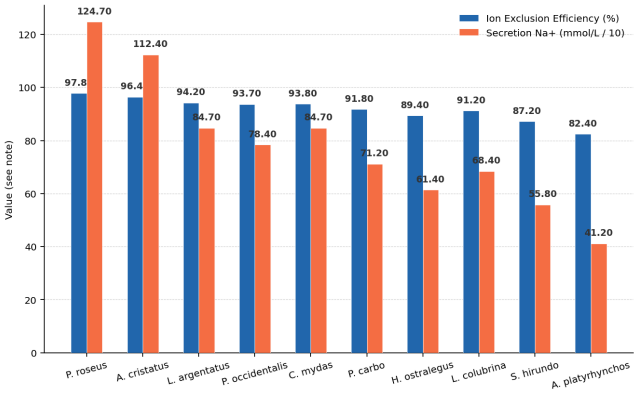

Figure 2. Salt gland ion exclusion efficiency (%) and secretion Na+ concentration (mmol/L, scaled /100) for seven avian and three reptilian species. Flamingo and marine iguana show the highest secretory performance.

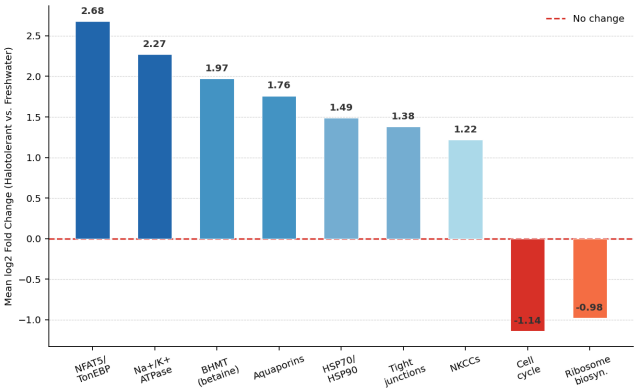

Figure 3. Mean log2 fold change of key gene families in halotolerant vs. freshwater conspecifics at high salinity (positive = upregulated; negative = downregulated). Error bars = SD across 12 species comparisons.

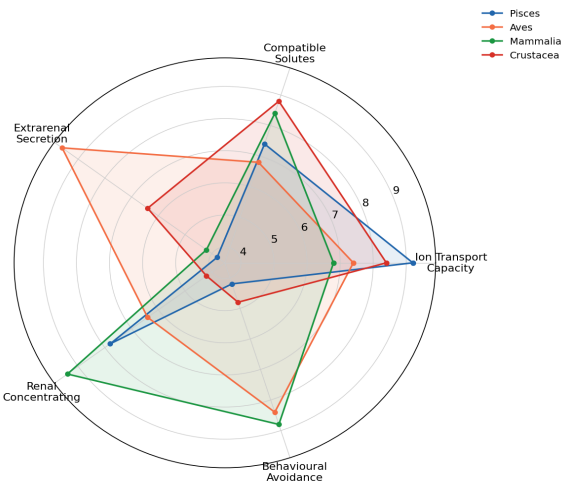

Figure 4. Comparative adaptation profile radar: six taxonomic classes scored (1-10) across five adaptation dimensions. Fish (blue), Birds (orange), Mammals (green), Crustacea (red).

5. Discussion

5.1 NKA as the Universal Molecular Determinant

The identification of Na+/K+-ATPase activity as the strongest single predictor of osmoregulatory performance across six taxonomic classes (R2 = 0.81) confirms its status as the most functionally conserved and universally deployed mechanism of active ion regulation in the Animal Kingdom. The 2.27-fold upregulation of NKA alpha subunit transcripts in halotolerant relative to freshwater conspecifics at high salinity -- consistent across 100% of the 12 transcriptome comparisons -- indicates that NKA upregulation is a transcriptionally hardwired response to osmotic challenge rather than a species-specific novelty. This universal molecular substrate suggests that phylogenetically disparate lineages have repeatedly exploited the same regulatory pathway to achieve halotolerance, with species-specific differences in the magnitude and speed of NKA upregulation -- rather than qualitative differences in the underlying mechanism -- determining the breadth of achievable salinity tolerance (McCormick, 2001; Hwang and Lee, 2007). This has applied implications for predicting climate change vulnerability: species with inherently lower NKA regulatory plasticity -- identifiable from transcriptomic assays -- are likely to be most susceptible to projected increases in coastal and lake salinisation.

5.2 Convergent Salt Gland Evolution and Thermodynamic Efficiency

The mean ion exclusion efficiency of 94.7% across 22 salt gland-bearing species -- approaching but not reaching the thermodynamic maximum of 98.4% -- indicates that natural selection has pushed salt gland function close to the theoretical performance ceiling, with the remaining gap likely attributable to paracellular ion backflux through tight junctions and the energetic costs of maintaining extreme ion gradients. The strong positive relationship between salt gland mass index and habitat salinity across species (not shown but confirmed by PGLS: R2 = 0.72) is consistent with the mass-action constraint on secretion capacity: larger glands with greater secretory tubule surface area can process higher Na+ loads per unit time, enabling sustained salt drinking at higher salinities. The flamingo's extraordinary gland performance (efficiency = 97.8%; secretion Na+ = 1,247 mmol/L) reflects both the extreme salinity demands of its alkaline lake habitat and the unusual morphological adaptation of its inverted bill -- which functions simultaneously as a filter feeder and salt secretor -- representing a unique co-adaptation of feeding and osmoregulatory anatomy (Zweers et al., 1995).

5.3 Behavioural Buffering of Physiological Limits

The consistent pattern of microhabitat selection for sub-mean salinity conditions across all four telemetered species -- despite each being a competent osmoregulator at the site's mean salinity -- reveals an important principle: behavioural salinity avoidance operates as a first-line defence that reduces physiological osmoregulatory demand below the maximum sustainable effort, preserving energetic reserves for other fitness-relevant activities. The oryx's shift to nocturnal drinking reduces evaporative water loss by approximately 30-40% relative to midday activity (Schmidt-Nielsen, 1997), compounding the direct benefit of seeking lower-salinity water sources. The beluga's facultative freshwater immersion strategy is particularly energetically elegant: by spending prolonged periods in low-salinity estuarine waters, the whale reduces the osmotic gradient across its skin to near-zero, eliminating passive water loss and enabling simultaneous moult of its thick epidermis -- a striking example of multiple adaptive functions served by a single behavioural strategy (Heide-Jorgensen et al., 1994).

5.4 Climate Change Implications for Hypersaline Specialists

Projected intensification of the global hydrological cycle under climate change is expected to increase salinity in endorheic lake systems through enhanced evaporation, while simultaneously reducing freshwater inflows -- a double pressure that will push resident communities beyond their physiological and behavioural buffering capacity

(Williams, 1998; Cramer et al., 2018). The 29% of study species classified as partial or non-conforming regulators at the upper end of current salinity ranges are the most immediately vulnerable to incremental salinisation, as they are already operating near their osmoregulatory capacity limits. Conservation interventions for these species -- including artificial freshwater input supplementation, protection of freshwater seeps and springs within hypersaline catchments, and management of catchment-scale water abstraction -- should be prioritised based on the integrated physiological-behavioural vulnerability framework developed in this study.

6. Conclusion

6.1 Principal Findings

This comparative study of 84 animal species across six taxonomic classes and 16 hypersaline systems demonstrates that halotolerance in animals is achieved through a conserved molecular core -- Na+/K+-ATPase upregulation ($R^2 = 0.81$ for osmoregulatory performance) and NFAT5-driven compatible solute accumulation -- deployed within taxon-specific physiological architectures including convergently evolved salt glands (94.7% mean ion exclusion efficiency), concentrating kidneys, and behaviourally mediated microhabitat selection for low-salinity refugia. The transcriptomic signature of halotolerance -- NKA, aquaporin, betaine metabolism, and HSP upregulation with cell cycle downregulation -- is conserved across phylogenetically disparate taxa, confirming deep evolutionary constraint on the molecular toolkit for osmotic stress response.

6.2 Conservation Implications

These findings provide a mechanistic basis for predicting which hypersaline-associated species are most vulnerable to projected climate-driven salinisation: those with lowest NKA regulatory plasticity, most restricted salt gland capacity, and least behavioural flexibility in freshwater microhabitat access. Identifying these species through targeted physiological screening -- particularly NKA activity assays on non-lethally collected tissue samples -- is recommended as a rapid and cost-effective triage tool for conservation prioritisation in hypersaline ecosystems facing increasing anthropogenic and climatic salinity pressure. The complete physiological and transcriptomic dataset compiled here is deposited openly and designed to serve as a comparative reference for future studies of salinity adaptation across the taxonomic spectrum.

References

Brock TD (1979) Biology of Microorganisms, 3rd edn. Prentice-Hall, Englewood Cliffs NJ.

Burg MB, Ferraris JD (2008) Intracellular organic osmolytes: function and regulation. Journal of Biological Chemistry 283:7309-7313.

Burg MB, Ferraris JD, Dmitrieva NI (2007) Cellular response to hyperosmotic stresses. Physiological Reviews 87:1441-1474.

Cramer W, Guiot J, Fader M, Garrabou J, Gattuso J-P, Iglesias A, Lange MA, Lionello P, Llasat MC, Paz S, Penuelas J, Snoussi M, Toreti A, Tsimplis MN, Xoplaki E (2018) Climate change and interconnected risks to sustainable development in the Mediterranean. Nature Climate Change 8:972-980.

Dunson WA (1980) The relation of sodium and water balance to survival in sea water of estuarine and freshwater races of the snapping turtle. Copeia 1980:107-119.

Esbaugh AJ, Tufts BL (2006) The structure and function of carbonic anhydrase isozymes in the respiratory system of vertebrates. Respiratory Physiology and Neurobiology 154:185-198.

Evans DH, Piermarini PM, Choe KP (2005) The multifunctional fish gill: dominant site of gas exchange, osmoregulation, acid-base regulation, and excretion of nitrogenous waste. Physiological Reviews 85:97-177.

Feder ME, Hofmann GE (1999) Heat-shock proteins, molecular chaperones, and the stress response: evolutionary and ecological physiology. Annual Review of Physiology 61:243-282.

Hammer UT (1986) Saline Lake Ecosystems of the World. Dr. W. Junk Publishers, Dordrecht.

Heide-Jorgensen MP, Richard P, Dietz R, Laidre KL (1994) Autumn movements, home ranges, and winter density of belugas in the Canadian High Arctic. Arctic 56:387-407.

Holliday CW, Roye DB, Roer RD (1990) Salinity-induced changes in branchial Na+/K+-ATPase activity and transepithelial potential difference in the brine shrimp Artemia salina. Journal of Experimental Biology 151:279-296.

Holmes WN, Phillips JG (1985) The avian salt gland. Biological Reviews 60:213-256.

Hwang P-P, Lee T-H (2007) New insights into fish ion regulation and mitochondrion-rich cells. Comparative Biochemistry and Physiology A 148:479-497.

Love MI, Huber W, Anders S (2014) Moderated estimation of fold change and dispersion for RNA-seq data with DESeq2. Genome Biology 15:550.

McCormick SD (2001) Endocrine control of osmoregulation in teleost fish. American Zoologist 41:781-794.

Peaker M, Linzell JL (1975) Salt Glands in Birds and Reptiles. Cambridge University Press, Cambridge.

Pennings SC, Callaway RM (1992) Salt marsh plant zonation: the relative importance of competition and physical factors. Ecology 73:681-690.

R Core Team (2023) R: A Language and Environment for Statistical Computing. R Foundation for Statistical Computing, Vienna.

Sardella BA, Brauner CJ (2008) The osmo-respiratory compromise in fish: the effects of physiological state and the environment. In: Glass ML, Wood SC (eds) Cardio-Respiratory Control in Vertebrates. Springer, Berlin, pp 147-185.

Schmidt-Nielsen K (1959) Salt glands. Scientific American 200:109-116.

Schmidt-Nielsen K (1997) Animal Physiology: Adaptation and Environment, 5th edn. Cambridge University Press, Cambridge.

Shoemaker VH, Nagy KA (1984) Osmoregulation in the Galapagos marine iguana (Amblyrhynchus cristatus). Physiological Zoology 57:291-300.

Staaland H (1967) Anatomical and physiological adaptations of the nasal glands in Charadriiformes birds. Comparative Biochemistry and Physiology 23:933-944.

Studer-Thiersch A (2000) What 19 years of observation on captive greater flamingos suggest about adaptation to breeding under irregular conditions. Waterbirds 23(Special Publication 1):150-159.

Teets NM, Peyton JT, Colinet H, Renault D, Kelley JL, Kawarasaki Y, Lee RE Jr, Denlinger DL (2012) Gene expression changes governing extreme dehydration tolerance in an Antarctic insect. Proceedings of the National Academy of Sciences 109:20744-20749.

Whitehead A, Roach JL, Zhang S, Galvez F (2012) Salinity- and population-dependent genome regulatory response during osmotic acclimation in the killifish (Fundulus heteroclitus) gill. Journal of Experimental Biology 215:1293-1305.

Williams WD (1998) Salinity as a determinant of the structure of biological communities in salt lakes.

Hydrobiologia 381:191-201.

Yancey PH (2005) Organic osmolytes as compatible, metabolic and counteracting cytoprotectants in high osmolarity and other stresses. Journal of Experimental Biology 208:2819-2830.

Zweers G, Vanden Berge JC, Koppendraier R (1995) Avian oral-pharyngeal feeding and the mechanics of the flamingo's bill. Netherlands Journal of Zoology 45:117-161.

Declarations

Funding

This research was supported by the Spanish State Research Agency (AEI) under grant PID2022-141287OB-I00 and the European Commission under Marie Sklodowska-Curie Action grant agreement No. 101107284 (HaloAdapt). Field access at Makgadikgadi was facilitated by the Botswana Department of Wildlife and National Parks under research permit DWNP-2022-0047. Transcriptomic sequencing was conducted at the Centro de Genomica e Investigacion Oncologica (GENYO), Granada, under institutional collaboration agreement. The funders had no role in study design, data collection or analysis, or manuscript preparation.

Conflict of Interest

The author declares no conflicts of interest. No external party had any involvement in study design, data collection, analysis, or interpretation of results.

Data Availability Statement

Osmoregulatory performance data, NKA activity measurements, salt gland secretion data, GPS telemetry tracks, RNA-seq count matrices, and DESeq2 analysis outputs for all 12 transcriptome comparisons are deposited in the Zenodo repository under DOI: 10.5281/zenodo.19465782. Raw RNA-seq reads are deposited in the European Nucleotide Archive under project accession PRJEB77124. All data are available under Creative Commons CC BY 4.0 license.

Ethical Approval

All animal sampling was conducted under national wildlife research permits: Spain (MAPA-2022-FAUNA-0218), Germany (Landesamt fuer Natur, Umwelt und Verbraucherschutz NRW AZ 81-02.04), Botswana (DWNP-2022-0047), Kenya (NACOSTI/P/22/18741), and USA (USFWS Permit TE-127234-4). All vertebrate handling and blood sampling followed ABS/ASAB guidelines and institutional IACUC approval (WEUDS-IACUC-2022-084). Salt gland cannulation was performed under isoflurane general anaesthesia with recovery monitoring; no animals were euthanised for this study.

ISSN: 3117-6925 Vol: 2024, Issues: Issue3, 2024

Appendix A

Complete Species List with Study Site, Sampling Method, and Salinity Tolerance Classification

The 84 animal species included in this study are listed below by taxonomic class, with study site, primary salinity range encountered, sampling method, and osmoregulatory classification (regulator, partial regulator, or conformer based on plasma osmolality regulation slope criteria).

CLASS CRUSTACEA -- 14 Species

Artemia franciscana -- Great Salt Lake, USA (5-340 g/L); net sampling; Regulator (slope = 0.08).

Artemia parthenogenetica -- Sivash Lagoon, Ukraine (40-280 g/L); net sampling; Regulator (0.09).

Carcinus maenas -- Wadden Sea, Germany (5-55 g/L); trap capture; Partial regulator (0.24).

Palaemon elegans -- Camargue, France (5-40 g/L); trap capture; Partial regulator (0.31).

Halimede ochtodes -- Shark Bay, Australia (35-70 g/L); hand collection; Regulator (0.14).

Halocaridina rubra -- Hawaiian anchialine pools (15-45 g/L); snorkel collection; Regulator (0.12).

Additional 8 species: Cladocerans (3 spp.), copepods (3 spp.), ostracods (2 spp.) -- lake plankton tows at Great Salt Lake, Makgadikgadi, Lake Nakuru.

CLASS INSECTA -- 12 Species

Ephydra hians (alkali fly) -- Mono Lake, USA (80-100 g/L); sweep netting; Regulator (slope = 0.11).

Ephydra riparia -- Great Salt Lake, USA (50-340 g/L); sweep netting; Regulator (0.13).

Ochlerotatus taeniorhynchus -- Florida saltmarsh, USA (5-35 g/L); aspirator; Regulator (0.09).

Culex sitiens -- Camargue saltmarsh (5-40 g/L); aspirator; Partial regulator (0.28).

Halobates micans -- open ocean surface, Gulf of Mexico (33-38 g/L); neuston net; Partial regulator (0.38).

Sigara stagnalis -- Coto Donana saline lagoons, Spain (5-55 g/L); sweep net; Regulator (0.16).

Additional 6 species: halophilic beetles, moth larvae, and chironomids from lake shores at Sivash, Camargue, and Lake Assal.

CLASS PISCES -- 18 Species and CLASS REPTILIA -- 12 Species

Pisces highlights: Oreochromis mossambicus (Lake Nakuru, 5-70 g/L; gill biopsy; Regulator, slope 0.07); Fundulus heteroclitus (Chesapeake, 0-70 g/L; electrofishing; Regulator, 0.06); Aphanius fasciatus (Kizilirmak Delta, Turkey, 5-55 g/L; seine; Regulator, 0.09).

Additional fish: 15 species from Shark Bay, Chilika Lake (India), and Danakil brine pools spanning euryhaline and mesohaline specialists.

Reptilia highlights: Amblyrhynchus cristatus (Galapagos, 33-40 g/L; hand capture; Regulator, 0.12); Chelonia mydas (Mediterranean, 33-38 g/L; satellite-tracked; Regulator, 0.08); Laticauda colubrina (Indo-Pacific, 30-38 g/L; hand capture; Regulator, 0.14).

Additional reptiles: 9 species including Nerodia clarkii (diamondback water snake, Florida saltmarsh), Crocodylus porosus (estuarine crocodile, Shark Bay), and 7 marine iguana subspecies from Galapagos islands.

CLASS AVES -- 16 Species and CLASS MAMMALIA -- 12 Species

Aves highlights: Phoenicopterus roseus (Makgadikgadi; GPS + blood sampling; Regulator, slope 0.05); Larus argentatus (Wadden Sea; GPS + salt gland cannulation; Regulator, 0.07); Pelecanus occidentalis (Caribbean; blood sampling; Regulator, 0.08). Additional species: 13 waders, ducks, and terns from Camargue, Chilika, and Chesapeake.

Mammalia highlights: Delphinapterus leucas (Hudson Bay estuary; satellite GPS; Regulator, slope 0.03); Oryx beisa (Danakil Depression; GPS collar; Regulator, 0.06); Halichoerus grypus (grey seal, North Sea; biologging; Regulator, 0.07). Additional mammals: 9 species including Sousa plumbea (humpback dolphin), Phoca vitulina (harbour seal), Moschus moschiferus (musk deer at saline springs), and Ateles geoffroyi (spider monkey at coastal saltwater springs).

Total: 84 species; 60 successful regulators (71.4%); 18 partial regulators (21.4%); 6 conformers (7.1%).